ISSN 1070-3284, Russian Journal of Coordination Chemistry, 2019, Vol. 45, No. 8, pp. 592–599. © Pleiades Publishing, Ltd., 2019.
Russian Text © The Author(s), 2019, published in Koordinatsionnaya Khimiya, 2019, Vol. 45, No. 8, pp. 504–512.

Dysprosium Thiocyanate Complexes with *s*-Triazine

S. P. Petrosyants[a, *], A. B. Ilyukhin[a], K. A. Babeshkin[a], E. V. Belova[a, b], A. V. Gavrikov[a], and N. N. Efimov[a]

[a] *Kurnakov Institute of General and Inorganic Chemistry, Russian Academy of Sciences, Moscow, 119991 Russia*

[b] *Moscow State University, Moscow, 119991 Russia*

**e-mail: petros@igic.ras.ru*

Received November 30, 2018; revised January 24, 2019; accepted January 28, 2019

Abstract—The reaction of $Dy(NCS)_3 \cdot 6H_2O$ with 2,4,6-tris(2-pyridyl)-*s*-triazine (Tptz) in MeOH, MeCN, and H_2O affords mononuclear neutral and ionic thiocyanate complexes with tridentate ligand Tptz: $[Dy(H_2O)(MeOH)(Tptz)(NCS)_3] \cdot Tptz$ (**I**), $[Dy(Tptz)_2(NCS)_3] \cdot MeCN$ (**II**), and $[Dy(H_2O)_3(Tptz)(NCS)_2] \cdot NCS \cdot Tptz \cdot 1.5H_2O \cdot 1.25MeOH$ (**III**). Structural features of the synthesized compounds are determined using powder XRD, IR spectroscopy, and thermoanalytical methods (thermogravimetry and differential scanning calorimetry). Compounds **II** and **III** exhibit the properties of single-molecule magnets.

Keywords: dysprosium thiocyanate, *s*-triazine, magnetic properties, single-molecule magnets

DOI: 10.1134/S1070328419080062

INTRODUCTION

The complexes of *f*-elements are most promising for the development of efficient single-molecule magnets (SMMs), coordination compounds retaining residual magnetization at the level of individual molecules for some time after switching the static magnetic field off. The unique magnetic properties of lanthanide ions caused by the intrinsic nature of *f* orbitals [1, 2] provide prospects for their use in the design of systems with improved magnetic properties. In turn, the known bistability of the ground state of Dy^{3+} (f^9) together with a significant magnetic anisotropy of this ion leads to the most probable (among all Ln^{3+}) manifestation of the SMM properties by coordination compounds of this lanthanide, namely, complexes of diverse structures (mono- and oligonuclear, as well as coordination polymers) with various core-forming ligands, the nature of which affects the composition and symmetry of the coordination environment of Ln^{3+} and, hence, the total magnetic anisotropy of the system. In particular, we have previously shown that the energy barriers of the magnetization reversal ($\Delta E/k_B$) for a series of mononuclear dysprosium(III) thiocyanates, namely, $Dy(NCS)_3 \cdot 6H_2O$, $[Dy(NCS)_3(H_2O)(Bipy)_2] \cdot 0.5(Bipy) \cdot H_2O$, $[Dy(NCS)_3(H_2O)(Phen)_2] \cdot Phen \cdot 0.5H_2O$, $[HBipy][Dy(NCS)_4(Bipy)_2] \cdot H_2O$, and $[HPhen][Dy(NCS)_4(Phen)_2]$, directly depend on the structural features of the compounds, mostly on the configuration of the coordination environment [3]. The reactions of hydrated thiocyanates $Ln(NCS)_3 \cdot 6H_2O$ (Ln = Y, Eu, Tb) with the polydentate ligand 2,4,6-tris(2-pyridyl)-*s*-triazine (Tptz) in various solvents (MeOH, MeCN, H_2O) were also described [4]. The possibility of preparing both neutral (for example, thiocyanate $[Y(H_2O)_2(Tptz)(NCS)_3]_2 \cdot Tptz \cdot 3.5H_2O$) and ionic complexes of the $[Y(H_2O)_3(Tptz)(NCS)_2] \cdot NCS \cdot Tptz \cdot 1.5H_2O \cdot 1.25MeOH$ type was established by means of single-crystal XRD and powder XRD [4]. Since the preparation of new Dy^{3+} complexes with the properties of efficient SMMs (SMM properties) unambiguously remains urgent, the study of complex formation in the corresponding systems similar to those described earlier [4] is of evident interest.

Herein, we studied the reaction of thiocyanate $Dy(NCS)_3 \cdot 6H_2O$ with the polydentate ligand Tptz. This assumed the synthesis of the mononuclear neutral (ionic) compounds with coordinated anions NCS^- and molecular ligands Tptz, H_2O, MeOH, and MeCN.

EXPERIMENTAL

Thiocyanate $Dy(NCS)_3 \cdot 6H_2O$ [3], Tptz (99%, Aldrich), and solvents (methanol, ethanol, and acetonitrile (high-purity grade)) were used as is. All experiments were carried out in air.

Synthesis of $[Dy(H_2O)(MeOH)(Tptz)(NCS)_3] \cdot Tptz$ (I). $Dy(NCS)_3 \cdot 6H_2O$ (0.1767 g, 0.40 mmol) in H_2O (5 mL) was added to a solution of Tptz (0.310 g, 0.99 mmol) in MeOH (25 mL) with stirring. A transparent olive-colored solution was poured to a cup for evaporation and left to stay in air at room temperature. The solid phase formed on the bottom of the cup was

separated next day on a paper filter. The yield was 0.15 g (37% based on Dy).

For $C_{40}H_{30}N_{15}O_2S_3Dy$ (*FW* = 1011.46)

Anal. calcd., %	C, 47.50	H, 2.99	N, 20.77	S, 9.51
Found, %	C, 48.91	H, 3.04	N, 21.16	S, 8.60

ATR-IR (ν, cm^{-1}): 3410 w, 3059 w, 2063 m, 2050 m, 1644 vw, 1596 vw, 1575 w, 1546 s, 1517 vs, 1491 m, 1470 m, 1434 m, 1403 w, 1385 m, 1374 s, 1300 w, 1255 m, 1151 w, 1095 w, 1051 w, 1007 m, 909 w, 861 m, 810 w, 766 vs, 739 m, 707 w, 666 s, 632 m, 490 m, 412 m.

Synthesis of $[Dy(Tptz)_2(NCS)_3] \cdot MeCN$ (II). Tptz (0.47 g, 1.50 mmol) was dissolved in MeOH (30 mL), and a solution of $Dy(NCS)_3$ (0.451 g, 1.01 mmol) in MeOH (30 mL) was added. A light yellow precipitate was almost immediately formed. The obtained suspension was stirred at room temperature for ~30 min and transferred onto a paper filter. The separated solid phase was washed with methanol and dried at room temperature. The yield of the solid precursor (P) was 0.68 g. A portion of product P was refluxed in MeCN for ~60 min. Compound **II** was filtered off from the obtained suspension.

For $C_{41}H_{25}N_{16}S_3Dy$ (*FW* = 1000.44)

Anal. calcd., %	C, 48.22	H, 2.51	N, 22.40	S, 9.62
Found, %	C, 47.94	H, 2.46	N, 21.06	S, 10.04

ATR-IR (ν, cm^{-1}): 3440 vw, 3063 w, 2075 m, 2055 s, 1587 w, 1575 w, 1546 s, 1514 vs, 1491 m, 1472 m, 1434 m, 1402 w, 1385 s, 1374 s, 1300 w, 1253 m, 1150 w, 1095 w, 1080 w, 1059 w, 1049 w, 1008 m, 993 w, 980 w, 909 vw, 861 w, 854 w, 810 vw, 766 vs, 741 m, 707 vw, 674 m, 666 s, 633 m, 622 w, 609 w, 490 m, 476 w, 443 w, 416 m.

Synthesis of $[Dy(H_2O)_3(Tptz)(NCS)_2] \cdot NCS \cdot Tptz \cdot 1.5H_2O \cdot 1.25MeOH$ (III). A portion of precursor P was dissolved on heating in a MeOH–MeCN (1 : 1) mixture (40 mL). The obtained yellow-greenish solution was kept for 24 h, and the formed solid phase was filtered off. The crystals of compound **III** isostructural to the similar yttrium complex [4] precipitated from the solution.

For $C_{40.25}H_{38}N_{15}O_{5.75}S_3Dy$ (*FW* = 1082.52)

Anal. calcd., %	C, 44.65	H, 3.53	N, 19.40	S, 8.88
Found, %	C, 44.37	H, 3.36	N, 19.99	S, 9.34

ATR-IR (ν, cm^{-1}): 3503 w, 3360 w, 3063 w, 2063 m, 2002 w, 1681 w, 1610 w, 1596 w, 1573 w, 1549 m, 1519 vs, 1493 m, 1471 m, 1434 m, 1386 m, 1372 s, 1304 w, 1259 m, 1178 w, 1151 w, 1095 w, 1052 w, 1007 m, 981 w, 916 w, 852 w, 814 w, 770 vs, 739 m, 674 m (sh), 666 s, 632 s, 566 m, 549 m, 524 m, 489 m, 479 m (sh), 467 m, 456 m, 446 m (sh), 419 m, 406 m.

Elemental analyses were carried out using standard procedures on a EURO EA 3000 CHN analyzer. Attenuated total reflectance infrared spectra (ATR-IR) were recorded in the range 4000–400 cm^{-1} on a Bruker ALPHA instrument (equipped with a diamond tool).

Powder X-ray diffraction analysis (XRD) was carried out on a Bruker D8 Advance diffractometer (CuK_α, Ni filter, LYNXEYE detector, reflection geometry). The Rietveld full profile refinement for the structures of compounds **II** and **III** was performed using the TOPAS program [5]. The cell parameters, profile parameters, background, predominant orientation, and scale factor were refined. The coordinates of atoms were taken from the isostructural yttrium compounds [4] and were not refined (Fig. 1, Table 1).

The thermal stability of the synthesized compounds was studied by differential scanning calorimetry (DSC) and thermogravimetry (TG) on NETZSCH DSC 204 F1 and NETZSCH TG 209 F1 instruments, respectively [6].

The magnetic behavior of complexes **II** and **III** were studied in the static and dynamic modes on a PPMS-9 (Quantum Design) magnetometer in the 2–300 K range. Magnetic fields with an intensity of 0–2000 Oe and an oscillation frequency of 10–10000 Hz were applied to study the dynamic magnetic susceptibility. In both cases, the intensity of the optimum magnetic field was 1000 Oe. The magnetic behavior was studied on polycrystalline milled samples sealed in polyethylene packages and frozen in a mineral oil in order to prevent field-induced orientation of crystallites [7]. The paramagnetic components of the magnetic susceptibility (χ) were determined taking into account both the diamagnetic contributions estimated from Pascal's constants and contributions from the mineral oil and sample holder.

RESULTS AND DISCUSSION

The neutral (**I**, **II**) and cationic (**III**) mononuclear complexes were isolated from the reaction of dysprosium aquathiocyanate with Tptz (ligand to metal ratio ≈ 2, reflux in methanol or acetonitrile). According to the obtained data, compounds **II** and **III** are isomorphous with the corresponding yttrium analogs [4]. In neutral complex **II**, the DyN_9 coordination node is formed by three NCS^- anions and two tridentately coordinated Tptz molecules.

A noticeable divergence between the calculated and experimental contents of C in complex **I** (47.50 versus 48.91%) originates from the synthesis conditions, namely, from the comparatively fast precipitation of the compound, which, most likely, led to the scavenging of the solvent molecules (MeOH). In the case of complex **II**, the experimentally determined content of N is lower than that calculated for the corresponding composition (22.40 vs. 21.06%) because

the very easy elimination of MeCN molecules of crystallization already during sample drying.

An impurity of $[Dy(H_2O)_3(Tptz)(NCS)_3]$ (**IIIb**) (6.6%) was found when refining the XRD pattern of compound **III**, and the coordinates of atoms for XRD analysis were taken from the isostructural Tb compound [8] (Table 1). In cationic complex **III**, the coordination sphere of Dy is formed by three O atoms of the water molecules and five N atoms of one Tptz ligand and two NCS. The outer sphere consists of water, methanol, and Tptz molecules as well as of one NCS.

Due to lack of single crystal XRD data for compound **I**, additional studies are necessary to refine the positions of the ligands in the coordination sphere. The IR spectrum of **I** exhibits a split band at 2063 and 2050 cm^{-1}, which is assigned to NCS- and is characteristic of all Ln thiocyanates. In addition, as in the case of the yttrium analogs [4], the IR spectrum of compound **I** contains intense bands of ν(C=C) and ν(C=N) vibrations of the Tptz ligand at 1546 and 1517 cm^{-1}, respectively. The presence of coordinated and outer-sphere Tptz molecules in the structure of compound **I** is confirmed by two distinctly discernible bands at 1374 and 1385 cm^{-1}, respectively.

The additional and unambiguous information about the composition and position of the ligands in the coordination sphere of compound **I** was obtained by the studies of solid-state thermolysis. Broad endoeffects are observed in the temperature range of −30–200°C on the DSC curves (Fig. 2, *a*) with a mass loss of 1.1% (Fig. 2, *b*). At these temperatures, the mass spectrum of evolved gases exhibits the peaks of the ionic current for *m/z*: 15 $\left[CH_3^+\right]$, 30 $[CH_2O^+]$, which are characteristic of methanol. Water, most likely, is also being removed in the same range, since the ionic currents for *m/z* (18 $[H_2O^+]$ and 17 $[OH^+]$) exceed the background level. Upon further heating, an exoeffect (39.0 J/g) at 208°C is observed on the DSC curves, and the mass loss is insignificant. It can be assumed that the heat evolution at this stage is due to the Tptz incorporation into the inner coordination sphere of complex **I** yielding an intermediate of the $[Dy(Tptz)_2(NCS)_3]$ (**IV**) composition. This assumption is confirmed by the results of comparative analysis of the IR spectra of the initial complex **I** and complex **IV**, since the spectrum of the intermediate, unlike that of complex **I**, contains only one well- resolved vibration band of the Tptz rings at 1375 cm^{-1}.

The autoindexing of the powder XRD pattern of product **IV** was performed using the DICVOL04 program [9]. The results of the full-profile refinement are presented in Fig. 1c and Table 1.

Thus, the possibility of the high-temperature incorporation of the initially outer-sphere Tptz molecule into the inner sphere of Ln^{3+} on heating the complexes of the $[Ln(H_2O)(MeOH)(Tptz)(NCS)_3] \cdot Tptz$ type is retained for the compounds of both light (Eu [4]) and heavy lanthanides.

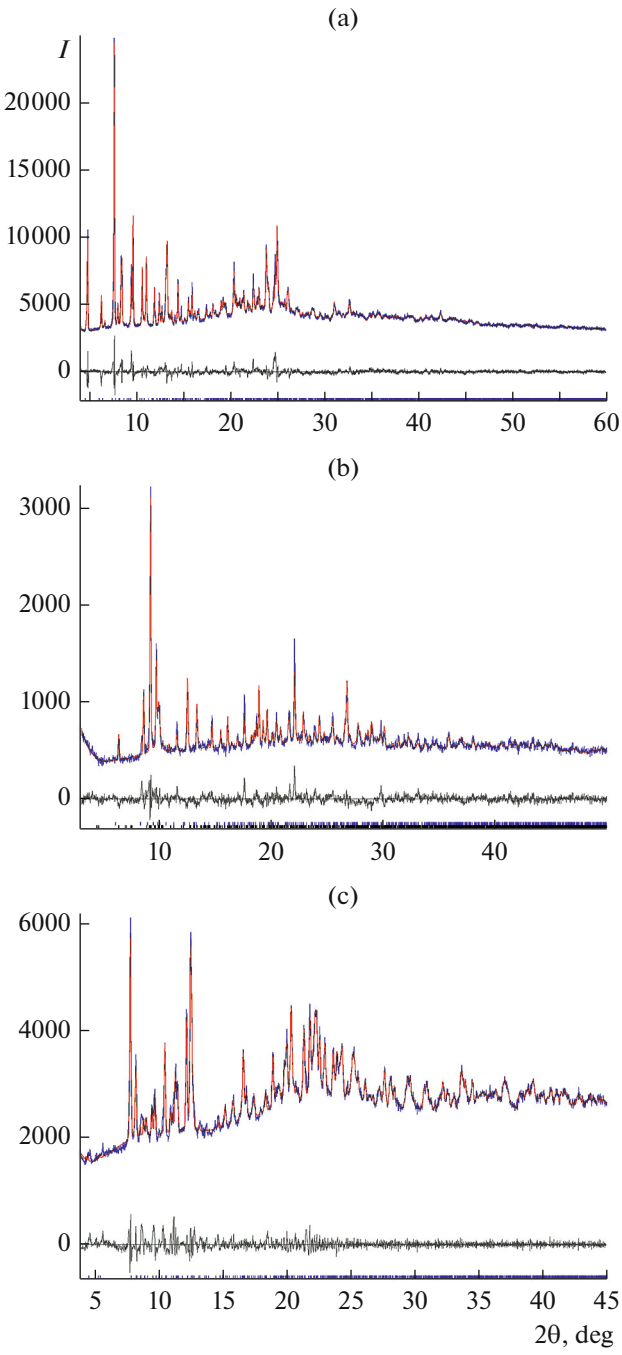

Fig. 1. Full-profile refinement of the structures of compounds (a) **II**, (b) **III**, and (c) **IV**.

The magnetic properties of compounds **II** and **III** were studied in the range of 2–300 K under a static magnetic field of 5000 Oe. The values of $\chi_m T$ (300 K) are 13.81 and 14.16 cm^3 K/mol (Fig. 3) for complexes **II** and **III**, respectively, and agree satisfactorily with

Table 1. Selected crystal data and structure refinement results for compounds **II–IV**

Parameter	Value			
	II	**III***	**IIIb***	**IV**
Crystal system	Triclinic	Monoclinic	Triclinic	Triclinic
Space group	$P\bar{1}$	$P2_1/c$	$P\bar{1}$	$P\bar{1}$
a, Å	14.5986(5)	10.6453(17)	13.60(10)	11.5313(13)
b, Å	15.2271(6)	19.7520(13)	21.23(10)	18.460(4)
c, Å	20.0463(14)	21.240(3)	19.73(22)	20.948(3)
α, deg	71.9507(6)	90	85.7(8)	112.175(11)
β, deg	85.050(5)	94.805(10)	76.8(11)	91.032(12)
γ, deg	82.939(4)	90	69.5(8)	103.036(11)
V, Å^3	4199.2(4)	4450.4(10)	5193(81)	3996.4(11)
Z	4	4	8	4
ρ_{calcd}, g/cm^3	1.59	1.61	1.78	
R_{Bragg}	1.779	3.365	1.790	
Range 2θ, deg	4–60	3–50		4–45
Increment 2θ, deg	0.02	0.02		0.02
Parameters	36	33		
R_{exp}	1.55	4.22		1.64
R_{wp}	3.83	6.46		3.03
R_p	2.62	4.96		2.07
GOOF	2.46	1.53		1.85

* Content in **III**–**IIIb** mixture = 93.4(9) : 6.6(9).

the theoretical value (14.17 cm^3 K/mol) for one isolated Dy^{3+} ($4f^9$, $^6H_{15/2}$, $g = 4/3$) [10]. The values of $\chi_m T$ for both the complexes decrease insignificantly with a temperature decrease to 100 K, whereas the decrease in $\chi_m T$ becomes more appreciable upon further cooling and reaches minimum values of 6.97 and 6.77 cm^3 K/mol at 2 K for complexes **II** and **III**, respectively. Such the cource of the dependences is typical of the Dy^{3+} complexes [3, 11–13]. Taking the proximity of the theoretical and experimental χT (300 K) values into account, one can conclude that the magnetic behavior of compounds **II** and **III** is virtually exclusively determined by the nature of Dy^{3+} under the given conditions.

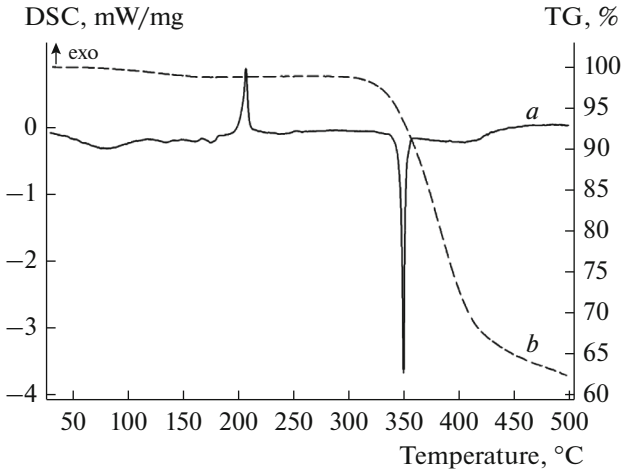

Fig. 2. (*a*) DSC and (*b*) TG curves for complex **I** on heating in an argon flow.

In order to establish the presence or absence of the SMM properties, we studied the magnetic behavior of compounds **II** and **III** in the dynamic mode, i.e., under alternating fields of various strength. In the zero magnetic field, only an insignificant increase in $\chi''(\nu)$ up to 0.12 cm^3/mol was observed in the case of complex **III** at the maximum attainable frequency of the used equipment $\nu = 10000$ Hz. This indicates some deceleration of the magnetization relaxation for complex **III**, but the absence of maxima in the $\chi''(\nu)$ dependences does not allow one to quantitatively determine the most important characteristics of the process. For complex **II**, no slow magnetic relaxation was observed under zero field

It is known that the application of an external magnetic field decreases the probability of quantum tunneling thus decreasing the relaxation rate. The measurements of the dynamic magnetic susceptibility in

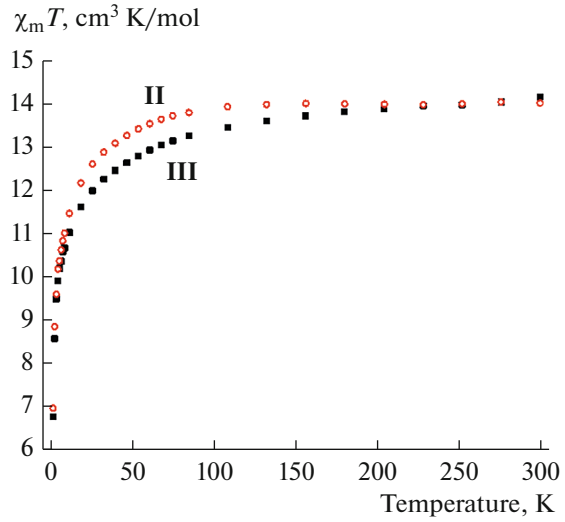

Fig. 3. $\chi_m(T)$ vs. T dependences for compounds **II** and **III** under a static magnetic field of 5000 Oe.

non-zero magnetic fields resulted in the appearance of a considerable signal on the imaginary components of the dynamic magnetic susceptibility of complexes **II** (Fig. 4) and **III** (Fig. 5). The variation of the external magnetic field intensity, H_{DC}, made it possible to determine the optimal field, the application of which allows the maximum on the corresponding $\chi''(\nu)$ dependences to be arranged at the lowest frequencies corresponding to the longest relaxation times. For both the complexes, optimal field is H_{DC} = 1000 Oe (Figs. 4, 5).

In order to determine the temperature dependences of the relaxation times under the optimal field, we measured the isotherms of the frequency dependences of the dynamic magnetic susceptibility in the ranges of 2–3.6 K (Fig. 6) and 2–7 K (Fig. 7) for complexes **II** and **III**, respectively. The relaxation times were determined from the positions of maxima on the frequency dependences of the imaginary magnetic susceptibility, $\tau = (2\pi\nu_{max})^{-1}$. Based on these data, we calculated the dependences of the relaxation time on the inverse temperature, $\tau(1/T)$, for complexes **II** and **III** (Fig. 8).

The high-temperature (3.6–3.4 K) region of the $\tau(1/T)$ dependence was approximated by the Arrhenius equation $\tau = \tau_0\exp(\Delta E/k_BT)$, which describes the Orbach relaxation process, in order to determine the relaxation parameters for complex **II**. The best approximation of the experimental data to the theoretical dependence was obtained at the preexponential factor $\tau_0 = 6.6 \times 10^{-8}$ s and the remagnetization barrier of the molecule $\Delta E/k_B$ = 21 K. The deviation of the $\ln\tau(1/T)$ dependence from linearity with the temperature increase indicates the effect of additional relaxation mechanisms. The approximation by the sum of several mechanisms was performed to reveal additional relaxation routes and to determine their parameters. The best fit of the experimental data and theoretical curve was achieved for the sum of the direct and Orbach relaxation mechanisms

$$\tau^{-1} = A_{direct}H^nT + \tau_0^{-1}\exp(-\Delta E/k_BT),$$

where A_{direct} and n are the parameters of the direct relaxation mechanism, T is temperature, τ_0 is the longest relaxation time, $\Delta E/k_B$ is the height of the energy barrier for the magnetization reversal, and k_B is the Boltzmann constant. The parameters obtained by the approximation in the entire temperature range (2–3.6 K) are as follows: $A_{direct} = 9.7 \times 10^{-10}$ s K^{-1} Oe^{-n}, n = 4.0, $\tau_0 = 1.1 \times 10^{-7}$ s, and $\Delta E/k_B$ = 20 K.

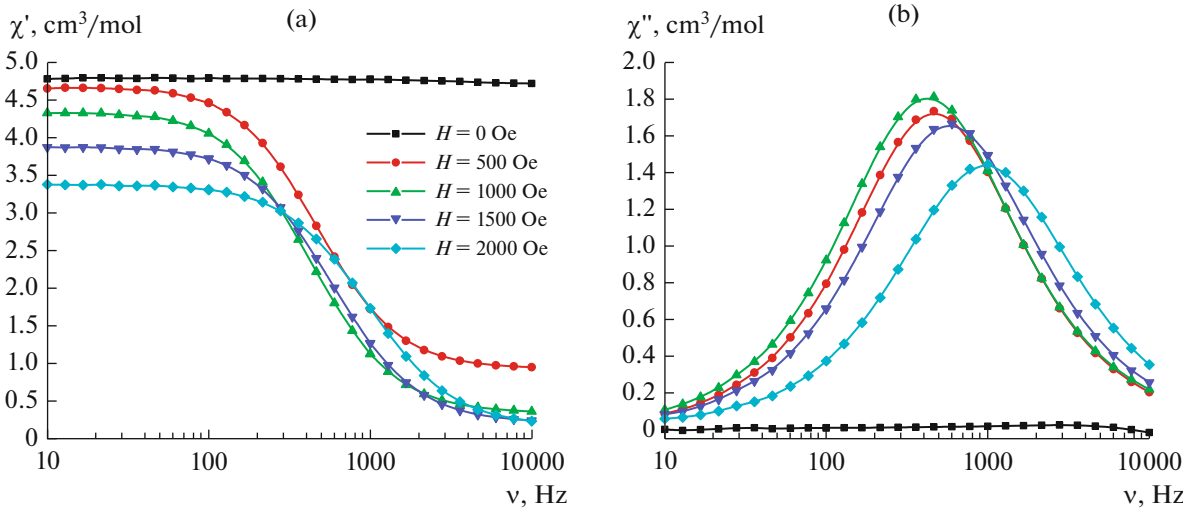

Fig. 4. Frequency dependences of the (a) real χ' and (b) imaginary χ'' components of the dynamic magnetic susceptibility of complex **II** at T = 2 K in magnetic fields of various intensities.

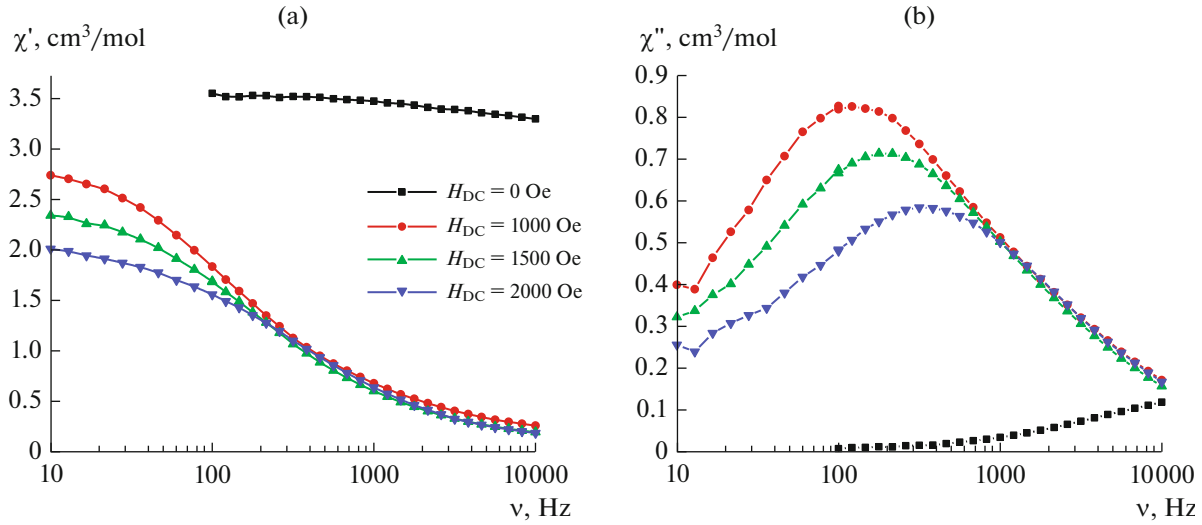

Fig. 5. Frequency dependences of the (a) real χ' and (b) imaginary χ" components of the dynamic magnetic susceptibility of complex **III** at $T = 2$ K in magnetic fields of various intensities.

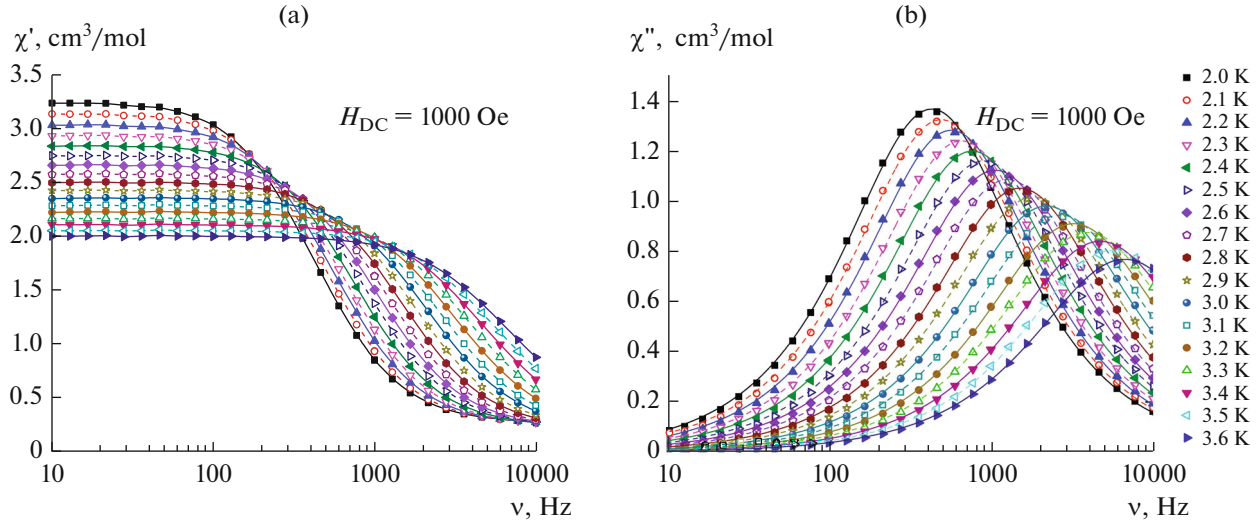

Fig. 6. Frequency dependences of the (a) real χ' and (b) imaginary χ" components of the dynamic magnetic susceptibility of complex **II** in the magnetic field with $H_{DC} = 1000$ Oe in the temperature range $T = 2$–3.6 K (lines are visual guides (a), approximation by the generalized Debye model (b)).

The maxima on the frequency dependences of the imaginary component of the dynamic magnetic susceptibility observed for complex **III** are noticeably broadened (Fig. 7), which may indicate the presence of an impurity of compound **IIIb** in the studied sample. The approximation of the high-temperature (5–3 K) region of the dependence of the relaxation time on the inverse temperature by the Arrhenius equation allowed one to estimate the fastest relaxation time $\tau_0 = 1.0 \times 10^{-6}$ s and the barrier of the magnetization reversal $\Delta E/k_B = 17$ K. At the same time, the approximation in the 2–7 K range, similarly to that for complex **II**, gave the results which are of physical sence only when the sum of the direct and Orbach relaxation mechanisms was involved. The best fitting parameters are as follows: $A_{direct} = 3.2 \times 10^{-10}$ s K^{-1} Oe^{-n}, $n = 4.0$, $\tau_0 = 5.9 \times 10^{-7}$ s, and $\Delta E/k_B = 19$ K.

It can be concluded that the $\Delta E/k_B$ values obtained using the sum of the direct and Orbach relaxation mechanisms are consistent with the ones obtained by the approximation of the high-temperature region by the Arrhenius equation. This fact indicates that the Orbach mechanism is main contributor to the relaxation of the molecule already at the temperatures higher than 3.4 K (for **II**) and 5 K (for **III**).

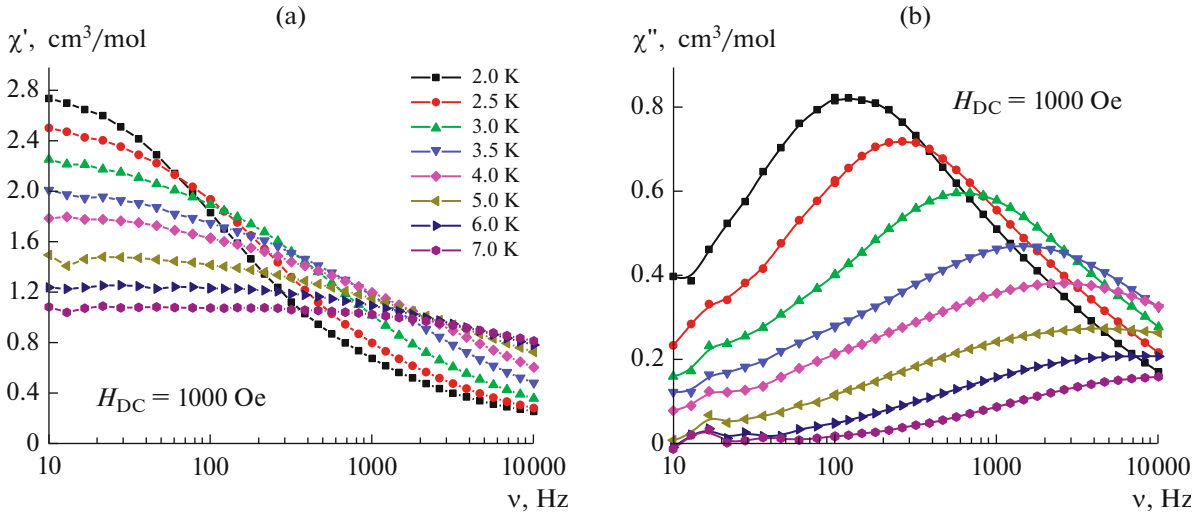

Fig. 7. Frequency dependences of the (a) real χ' and (b) imaginary χ" components of the dynamic magnetic susceptibility of complex **III** in the magnetic field with H_{DC} = 1000 Oe in the temperature range T = 2–7 K (lines are visual guides (a), approximation by the generalized Debye model (b)).

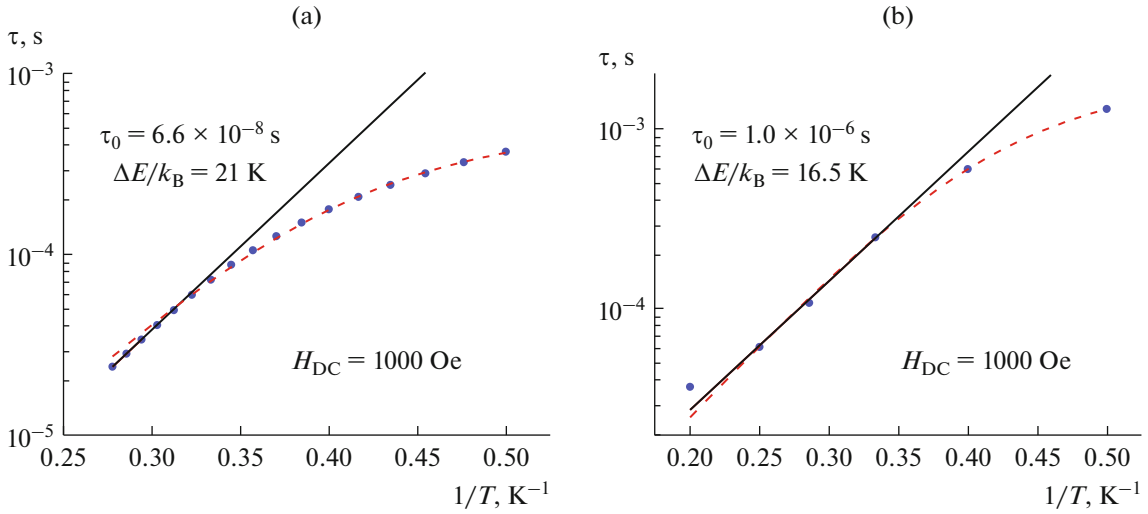

Fig. 8. Relaxation time vs. inverse temperature dependences for complexes (a) **I** and (b) **II** under the optimal magnetic field H_{DC} = 1000 Oe. The solid line is the approximation of the high-temperature region (T = 3.6–3.4 (**II**), 5–3 K (**III**)) by the Arrhenius equation, and dashed line is the approximation by the sum of the direct and Orbach relaxation mechanisms.

Thus, complexes **II** and **III** are new representatives of so-called field-induced SMMs, i.e., demonstrate the substantially decelerated relaxation of magnetization upon the application of static magnetic fields.

Taking into account our previous results of studying the thiocyanate SMMs with the bidentate N-donor ligands Bipy and Phen which are of similar nature with Tptz [3], we can assume that an increase in the denticity of such ligands results in the significant deterioration of the SMM properties. In fact, for previously studied $[Dy(NCS)_3(H_2O)(Bipy)_2] \cdot 0.5(Bipy) \cdot H_2O$ and $[Dy(NCS)_3(H_2O)(Phen)_2] \cdot Phen \cdot 0.5H_2O$ [3], the values of $\Delta E/k_B$ are 28 and 27 K, respectively. This assumption is additionally confirmed by the results of studying the $[Dy(NCS)_3(Terpy)_2]$ complex involving another tridentate N-donor ligand similar in structure, namely: 2,2';6',2"-terpyridine (Terpy) [14]. Only the fact of somewhat decelerated relaxation of magnetization can be established for this compound even when static magnetic fields of various strength are applied, but the determination of the most important characteristics of the process ($\Delta E/k_B$ and τ_0) is impossible. The obtained results confirm the previously revealed theoretical trends of the influence of the geometry of the coordination environment on the SMM properties of the Dy heteroleptic thiocyanate

complexes [15]. Indeed, the geometric rigidity of the tridentate ligands Tptz and Terpy [14] evidently makes it impossible to accomplish the sandwich geometry of the coordination environment, which was shown to be favorable for the manifestation of the SMM properties of the Dy complexes [15].

To conclude, the results obtained herein as well as the published data for the thiocyanate complexes of rare-earth elements with heterocyclic polydentate N-donor ligands [3, 16, 17] indicate a tendency for such the complexes to form compounds with both inner- and outer-sphere ligand molecules. The transition of the polydentate N-donor ligand from the exo- to endo-coordination mode occurs with a temperature increase, and the characteristics of the process are determined by the nature of both the Ln^{3+} ion (primarily, ionic radius) and organic ligand (steric features). In addition, the known results of studying similar complexes as SMMs indicate the negative effect of an increase in the denticity of the additional N-donor ligand on the parameters of the slow magnetic relaxation.

ACKNOWLEDGMENTS

This research was performed using the equipment of the JRC PMR IGIC RAS.

FUNDING

This work was supported by the Russian Science Foundation, project no. 16-13-10407. Elemental analyses of the complexes were supported by IGIC RAS state assignment.

REFERENCES

1. Huang, Ch., *Rare Earth Coordination Chemistry: Fundamentals and Applications*, Singapore: Wiley, 2010.
2. Wang, B., Jiang, S., Wang, X., and Gao, S., in *Rare Earth Coord. Chem. Fundamentals and Applications*, Huang, Ch., Ed., Willey (Asia) Pte Ltd., 2010, pt 9, p. 355.
3. Petrosyants, S.P., Dobrokhotova, Zh.V., Ilyukhin, A.B., et al., *Eur. J. Inorg. Chem.*, 2017, p. 3561.
4. Petrosyants, S.P., Ilyukhin, A.B., Gavrikov, A.V., and Efimov, N.N., *Russ. J. Coord. Chem.*, 2018, vol. 44, no. 12, p. 745. https://doi.org/10.1134/S1070328418120060
5. TOPAS, Karlsruhe: Bruker AXS, 2005.
6. Ilyukhin, A.B., Dobrokhotova, Zh.V., Petrosyants, S.P., and Novotortsev, V.M., *Polyhedron*, 2011, vol. 30, no. 16, p. 2654.
7. Petrosyants, S.P., Ilyukhin, A.B., Efimov, N.N., and Novotortsev, V.M., *Russ. J. Coord. Chem.*, 2018, vol. 44, no. 11, p. 660. https://doi.org/10.1134/S1070328418110064
8. Goel, N., *J. Coord. Chem.*, 2015, vol. 68, no. 3, p. 529.
9. Boultif, A. and Louër, D., *J. Appl. Crystallogr.*, 2004, vol. 37, no. 5, p. 724.
10. Benelli, C. and Gatteschi, D., *Chem. Rev.*, 2002, vol. 102, p. 2369.
11. Gavrikov, A.V., Efimov, N.N., Dobrokhotova, Zh.V., et al., *Dalton Trans.*, 2017, vol. 46, p. 11806.
12. Gavrikov, A.V., Efimov, N.N., Ilyukhin, A.B., et al., *Dalton Trans.*, 2018, vol. 47, p. 6199.
13. Gavrikov, A.V., Koroteev, P.S., Efimov, N.N., et al., *Dalton Trans.*, 2017, vol. 46, p. 3369.
14. Petrosyants, S.P., Ilyukhin, A.B., Gavrikov, A.V., et al., *Inorg. Chim. Acta*, 2019, vol. 486, p. 499.
15. Rinehart, J.D. and Long, J.R., *Chem. Sci.*, 2011, vol. 2, p. 2078.
16. Petrosyants, S.P., Ilyukhin, A.B., Dobrokhotova, Zh.V., et al., *Russ. J. Coord. Chem.*, 2017, vol. 43, no. 6, p. 352. https://doi.org/10.1134/S1070328417060057
17. Dobrokhotova, Zh.V., Petrosyants, S.P., Ilyukhin, A.B., et al., *Inorg. Chim. Acta*, 2017, vol. 456, p. 76.

Translated by E. Yablonskaya